

Date 2010
Author Bogaert, H., L. Brosset and M.L. Kaminski

Address Delft University of Technology
Ship Hydromechanics Laboratory
Mekelweg 2, 2628 CD Delft



Delft University of Technology

**Intercation between wave impacts and
Corrugations of MarkIII Containment
System for LNG Carriers: findings from
The SlosheI project
by**

H. Bogaert, L. Brosset and M.L. Kaminski

Report No. 1721-P

2010

**Published in: Proceedings of the 20th International
Offshore and Polar Engineering Conference, Beijing,
China, June 20-25, 2010, ISOPE'10,
ISBN: 978-1-880653-77-7**

The Proceedings of The Twentieth (2010) International OFFSHORE AND POLAR ENGINEERING CONFERENCE

Beijing, China, June 20-25, 2010

VOLUMES 1~4, 2010

ISBN 978-1-880653-77-7 (Vols. 1-4 Full Proceedings Set)

ISSN 1098-6189 (Vols. 1-4 Full Proceedings Set)

Indexed by **Engineering Index, EI Compendex** and Others

www.isopec.org

orders@isopec.org



ISOPE International Society of
Offshore and Polar Engineers

The Proceedings of The Twentieth (2010) International OFFSHORE AND POLAR ENGINEERING CONFERENCE

Beijing, China, June 20-25, 2010

VOLUME I, 2010

FRONTIER ENERGY RESOURCES TECHNOLOGY

LNG and Process, Clean Energy, Gas Hydrates, Ocean Resources and Technology

SOUTH CHINA SEA AND SUBSEA

MetOcean and Subsea, Subsea Flows, Assurance and Measurements

DEEPWATER INSTALLATION , OFFSHORE MECHANICS AND TECHNOLOGY

Shipbuilding Industry Model, Jacket and Jackup, Floating Structures and FPSO and SPAR, Offshore Systems and Design

RENEWABLE ENERGY AND ENVIRONMENT

Wind Energy, Tidal Energy and OTEC, Wave Energy, Wind Energy: International Progress

ENVIRONMENT SCIENCE AND ENGINEERING

Environment Modeling, Monitoring and Assessment, Biochemistry and Plankton, Oil Spill in Offshore and Ice Storage and Diffusion

ARCTIC SCIENCE AND TECHNOLOGY

Pack Ice, Ice Process, Ice-Structure Interactions, Polar Ocean Environment, Ice Forecasting, Polar Shipping

How to Use This Table of Contents

Scroll down or use the links in the left-side frame to move to a new location in this index.

To locate a specific paper title in the Table of Contents, click **Ctrl-F** on the keyboard to activate the **FIND** feature, and then "FIND" window will open. Type in your "search word" and it will find the word and paper title on that content page. Click on a **blue paper title** you like to view.

To return to this index after viewing a paper, click on the appropriate "Volume" link in the left-side frame.

This CD-ROM was created from the author-made PDF files. View quality of the text and graphics and the ease of readability depend largely on the quality and/or consistency of the PDF-making procedure the authors used.

ISBN 978-1-880653-77-7 (Vols. 1-4 Full Proceedings Set)

ISSN 1098-6189 (Vols. 1-4 Full Proceedings Set)

Indexed by **Engineering Index, EI Compendex** and Others

www.isopec.org

orders@isopec.org

Edited by:

Jin S. Chung, ISOPE, Cupertino, California, USA

Raghavan Ayer, ExxonMobil Research and Engineering Company, Annandale, New Jersey, USA

Simon Prinsenber, Bedford Institute of Oceanography, Dartmouth, Canada

Seok Won Hong, Maritime and Ocean Engineering Research Institute, Daejeon, Korea

Ivar Langen, University of Stavanger, Stavanger, Norway

Presented at:

The Twentieth (2010) International Offshore and Polar Engineering Conference held in Beijing, China, June 20-25, 2010

Organized by:

International Society of Offshore and Polar Engineers

Sponsored by:

International Society of Offshore and Polar Engineers (ISOPE) with cooperating societies and associations

The publisher and the editors of its publications assume no responsibility for the statements or opinions expressed in papers or presentations by the contributors to this conference or proceedings.

International Society of Offshore and Polar Engineers (ISOPE)

P.O. Box 189, Cupertino, California 95015-0189 USA

CONTENT

PLENARY PRESENTATIONS

Korean Shipbuilding Industry Growth and its Future Challenges	1
Dong Shik Shin	
Latest Progress in Floatover Technologies for Offshore Installations and Decommissioning	9
Alan M. Wang, Xizhao Jiang, Changsheng Yu, Shaohua Zhu, Huailiang Li and Yungang Wei	
SECOND FRONTIER ENERGY RESOURCES TECHNOLOGY SYMPOSIUM	
LNG and Process	
Dynamic Behavior of LNG Storage Tank During Leakage Conditions	21
HD Wei, MZ Zhou, YC Zhang, J Su, SZ Yan, JC Wang and S Yang	
Selection and Simulation of Offshore LNG Liquefaction Process	25
Jianlu Zhu, Yuxing Li, Yonghao Liu and Weiwei Wang	
Design Development of BOG Handling System in LNG-FSRU	33
Youngsoon Sohn, Donghyuk Kim, Sunghye Choi and Youngmyung Yang	
Clean Energy	
Advancement of Direct Coal Liquefaction	37
Tan-Ping Chen	
Coal Drying by a Pneumatic Conveying System	41
Kyoungsoo Lim, Sangdo Kim, Sihyun Lee and Soonkwan Jeong	
Numerical Analyses and Engineering Calculations for the Conceptual Design of Compact Gasifier	46
Jin-Wook Lee, Seok-Woo Chung, Ryeo-Hwa Heo, Yongseung Yun and Seong-Hun Choi	
Opportunities for Coal-to-Gas in China	51
Azfar Shaukat and Martin Tai	
CO₂-Sorption Enhanced Reaction for the Production of High-Purity Hydrogen from Synthesis Gas Produced by Coal Gasification	58
Ki Bong Lee, Jung Moo Lee, Sang Goo Jeon, Jeong Geol Na and Ho Jung Ryu	
Study of Optimal Operating Conditions in the Partitioned Fluidized Bed Gasifier Using a Commercial Simulator	64
Young Cheol Park, Seung-Yong Lee, Sung-Ho Jo, Jong-Ho Moon and Gyoung Tae Jin	
A Study of the Gasification Characteristics in a Partitioned Fluidized Bed	67
Gyoung Tae Jin, Seung-Yong Lee, Young Cheol Park, Sung-Ho Jo, Jong-Ho Moon and Ho-	

Measuring the Groundwater Level Using a Hole of the Swedish Weight Sounding Test	789
C. Kim, K. Tei and M. Fujii	
Old Ridge Road Used as the Fail-safe Path	793
Youji Nakane, Masao Okuda, Yukihiro Kani and Kiyoshi Hayakawa	

The Proceedings of The Twentieth (2010) International OFFSHORE AND POLAR ENGINEERING CONFERENCE

Beijing, China, June 20-25, 2010

VOLUME III, 2010

SLOSHING DYNAMICS AND DESIGN

LNG Sloshing, LNG Sloshing: GTT, LNG Sloshing: Sloshel, LNG Sloshing: Physics, LNG Sloshing: CFD, LNG Ship Motion, Tank Sloshing and Sloshing Loads

HYDRODYNAMICS

Ocean Waves, Freak and Tsunami Waves, Wave Loading and Slamming, Floating Bodies, CFD-NWT, CFD-Particle Method, CFD

COASTAL ENGINEERING

Coastal Waves, Wave Breaking, Seabed and Sediment Transport, Tsunami and Storm Surge, Breaking Waves and Wave Force, Tidal Characteristics and Estuary, Port and Harbor, Breakwaters and Dikes, Beach Evolution

FLOW-INDUCED VIBRATIONS

How to Use This Table of Contents

Scroll down or use the links in the left-side frame to move to a new location in this index.

To locate a specific paper title in the Table of Contents, click **Ctrl-F** on the keyboard to activate the **FIND** feature, and then "FIND" window will open. Type in your "search word" and it will find the word and paper title on that content page. Click on a **blue paper title** you like to view.

To return to this index after viewing a paper, click on the appropriate "Volume" link in the left-side frame.

This CD-ROM was created from the author-made PDF files. View quality of the text and graphics and the ease of readability depend largely on the quality and/or consistency of the PDF-making procedure the authors used.

ISBN 978-1-880653-77-7 (Vols. 1-4 Full Proceedings Set)

ISSN 1098-6189 (Vols. 1-4 Full Proceedings Set)

Indexed by **Engineering Index, EI Compendex** and Others

www.isopec.org

orders@isopec.org

Edited by:

Jin S. Chung, ISOPE, Cupertino, California, USA

Frederic Dias, Ecole Normale Supérieure-Cachan, Cachan, France

Jui-Fang Kuo, ExxonMobil Upstream Research Company, Houston, TX, USA

Qingwei Ma, The City University, London, UK

Presented at:

The Twentieth (2010) International Offshore and Polar Engineering Conference held in Beijing, China, June 20-25, 2010

Organized by:

International Society of Offshore and Polar Engineers

Sponsored by:

International Society of Offshore and Polar Engineers (ISOPE) with cooperating societies and associations

The publisher and the editors of its publications assume no responsibility for the statements or opinions expressed in papers or presentations by the contributors to this conference or proceedings.

International Society of Offshore and Polar Engineers (ISOPE)

P.O. Box 189, Cupertino, California 95015-0189 USA

CONTENT

SECOND ISOPE SLOSHING DYNAMICS AND DESIGN SYMPOSIUM

LNG Sloshing

Methodology for LNG Terminals	1
Louis Diebold	
Experimental and Numerical Investigations of the Global Forces Exerted by Fluid Motions on LNGC Prismatic Tanks Boundaries	10
Nicolas Moirod, Eric Baudin, Thomas Gazzola and Louis Diebold	
Development of a New Reduction Device of Sloshing Load in Tank	18
Yousuke Anai, Takahiro Ando, Naohiko Watanabe, Chikahisa Murakami and Yoshiteru Tanaka	
Structural Response of the Insulation Box on NO96 Membrane Containment System	26
Hirotsugu Dobashi and Akio Usami	

LNG Sloshing: GTT

Sloshing and Scaling: Experimental Study in a Wave Canal at Two Different Scales	33
O. Kimmoun, A. Ratouis and L. Brosset	
Simulation of Liquid Impacts with a Two-phase Parallel SPH Model	44
P.-M. Guilcher, G. Oger, L. Brosset, E. Jacquin, N. Grenier and D. Le Touzé	
On the Effect of Phase Transition on Impact Pressures due to Sloshing	53
J.-P. Braeunig, L. Brosset, F. Dias and J.-M. Ghidaglia	
Comparative Study of FE Models of LNG Containment System NO.96	62
A. Arswendy, Oddgeir Liasjoe and Torgeir Moan	
The Effect of Inner Steel Hull Flexibility on the Responses of the LNG Containment System No.96 under Static Loads	69
A. Arswendy, Oddgeir Liasjoe and Torgeir Moan	

LNG Sloshing: SlosheI

Full Scale Sloshing Impact Tests - Part 2	76
Mirosław Lech Kaminski and Hannes Bogaert	
Sloshing and Scaling: Results from the SlosheI Project	88
H. Bogaert, S. Léonard, L. Brosset and M.L. Kaminski	
Hydro-structural Behaviour of LNG Membrane Containment Systems under Breaking Wave Impacts: Findings from the SlosheI Project	98

H. Bogaert, S. Léonard, M. Marhem, G. Leclère and M. Kaminski

Interaction Between Wave Impacts and Corrugations of MarkIII Containment System for LNG Carriers: Findings from the SlosheI Project 109

H. Bogaert, L. Brosset and M.L. Kaminski

Validation of Numerical Tools for LNG Sloshing Assessment 119
X.Zheng, J R Maguire and D Radosavljević

LNG Sloshing: Physics

On the Effect of Compressibility on the Impact of a Falling Jet 129
Paul Christodoulides, Frédéric Dias, Jean-Michel Ghidaglia and Marc Kjerland

Experimental Study of Evolution of Impact Pressure along the Vertical Walls of a Sloshing Tank 137
N. Repalle, F. Pistani and K. Thiagarajan

A Study on Flow Field around Membrane Corrugation 142
DW Kwak, JY Chung, SH Kwon and SH Oh

Set-up of a Sloshing Laboratory at the University of Western Australia 147
F. Pistani, K. Thiagarajan, R. Seah and D. Roddier

Sloshing Response of LNG Tanks Subjected to Seismic Ground Motion 154
Juan Su, Meizhen Zhou, Jianxing Yu and Huidong Wei

LNG Tank Sloshing Parameter Study in a Multi-Tank Configuration 161
André Baeten

Seismic Response of LNG Storage Tank under Different Base Conditions and Liquid Height 169
Kangwon Lee, Jun Hwi Kim and Heung Seok Seo

Sloshing Load due to Liquid Motion in a Tank Comparison of Potential Flow, CFD, and Experiment Solutions 174
Yusong Cao, Mateusz Graczyk, Csaba Pakozdi, Haidong Lu, Fuxin Huang and Chi Yang

LNG Sloshing: CFD

Numerical Simulation of Liquid Sloshing in LNG Containers 186
Yuxing Li, Fafeng Sun, Wuchang Wang, Xichong Yu and Leilei Zang

Numerical Simulation of 2D Sloshing by using ALE2D Technique of LS-DYNA and CCUP Methods 192

Interaction between wave impacts and corrugations of MarkIII Containment System for LNG carriers: findings from the SlosheI project

H. Bogaert^(1,2), L. Brosset⁽³⁾, M.L. Kaminski⁽¹⁾

¹MARIN, Hydro Structural Services, Wageningen, The Netherlands

²Delft University of Technology, Ship Structures Laboratory, Delft, The Netherlands

³GTT (Gaztransport & Technigaz), Liquid Motion Department, Saint-Rémy-lès-Chevreuse, France

ABSTRACT

The subject of this paper is the behavior of MarkIII corrugated primary membrane under breaking wave impacts. The study is based on the database of the *large scale impact tests* from the *SlosheI* project. Unidirectional breaking waves were generated in a flume tank in order to break onto an instrumented wall covered by a corrugated surface reproducing the MarkIII membrane at scale 1:6. Pressure sensors were positioned in between the corrugations. A special sensor was designed to measure the net force in the upward and downward direction on a horizontal corrugation. Special care was taken to observe the interaction between the wave impact and the corrugations by high speed cameras synchronized with the data acquisition system.

Four sources of impact loads on the corrugations were observed: the wave trough, the wave crest, the jet formed after wave impact or the entrapped air. This observation gave evidence that more mechanisms are involved during sloshing-corrugation interaction than those identified previously with wet drop tests. Moreover, the pressure measured upstream and downstream of a horizontal corrugation is correlated to the global vertical force, but this relation depends highly on the sensor position with regards to the corrugation, and the source of loading.

The paper describes the different kinds of corrugation loadings during breaking wave impacts. It emphasizes the need to take into account the sloshing corrugation interaction into a sloshing assessment methodology but shows that applying scaled corrugations in small scale tests (scale around 1:40 - 1:35) is not adequate.

KEY WORDS: sloshing, LNG carrier, membrane containment system, MarkIII, corrugation, impact pressure, model test, flume tank, breaking wave.

INTRODUCTION

MarkIII is one of the membrane Cargo Containment Systems (CCS) designed by GTT for LNG carriers. It is mainly composed of 3 m x 1 m panels of polyurethane foam covered by a stainless steel corrugated membrane in contact with the LNG at -162°C (see Figure 1). The panels are bonded to the double hull by resin ropes.

The membrane features large parallel corrugations crossing perpendicularly small parallel corrugations. The large and small corrugations are respectively 54 mm and 37.2 mm high. The distance between two large or two small corrugations is 340 mm. On the

longitudinal walls of the MarkIII tanks the large corrugations are vertical whilst they are horizontal on the transverse bulkheads.

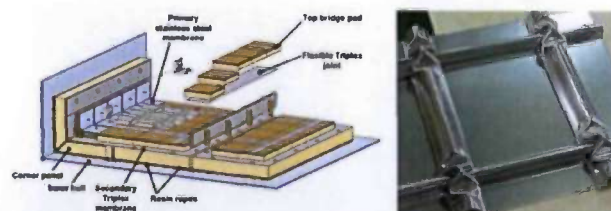


Figure 1 – MarkIII containment system (left), sample of the corrugated membrane (right)

In 2008, some deformations of the membrane corrugations were observed for the first time on board several MarkIII ships during routine dry dock inspections. These deformations, without any leakage of the cargo, affected both large and small corrugations mainly in the corners of the ceiling and less frequently in the region covering a few meters above the chamfers of the longitudinal bulkheads. They had clearly been caused by sloshing impacts. Some corrugations were globally bent whereas some others were pinched almost symmetrically.

The design loads on the CCS of membrane ships are determined by using a sloshing assessment methodology based on model tests with tanks at scale 1:40 and flat walls (see Gervaise *et al.*, 2009). After these incidents some questions were raised:

- How to determine the loads on the corrugations?
- Could the presence of corrugations magnify the loads locally on the polyurethane foam?
- How to take this influence into account within the methodology? Is it relevant to have scaled corrugations inside the model tanks?

After the incidents an investigation plan was launched by GTT. A reverse engineering process permitted to evaluate the loads capable of producing the different deformations observed. It was concluded that, with a static pressure up to 20 bar, both the corrugations and the insulation below remain sound, even though the corrugations may be significantly deformed.

The analysis presented in this paper was carried out based on experimental results from the *SlosheI* project (see Brosset *et al.*, 2009). So-called *large scale tests* were carried out by MARIN in the *Scheldt* flume of Deltares (NL). Unidirectional breaking waves were generated in the flume in order to impact an instrumented rigid vertical wall. Two configurations of the wall were tested: a flat wall and a corrugated wall

reproducing at scale 1:6 the MarkIII membrane as arranged on longitudinal bulkheads (large corrugations are set vertically).

The paper explains the main findings from these experiments and gives partial answers to the above mentioned questions raised after the incidents. The answers brought here are considered as partial for two main reasons:

- Wave impacts studied are much idealized compared to 3D sloshing events and are only representative of sloshing impacts for low and partial filling conditions. As they are unidirectional they are not relevant to understand bending deformations of the vertical corrugations.
- The tests were performed at scale 1:6. Full scale wave impact tests with the MarkIII containment system have been just completed in April 2010 within SlosheL project. The conclusions from the large scale tests will be up-dated as soon as the full scale data are analysed.

SLOSHEL LARGE SCALE TEST SET-UP

At the time of testing, the *Scheldt* flume was 55 m long, 1.5 m high and 1 m wide. The flume could be filled up to 1.0 m. The flume walls were transparent. A piston wave maker was installed at an end of the flume. A rigid test wall was installed at 23.7 m from the paddle. The test wall and the whole set-up is detailed by Bogaert and Kaminski (2010). The test set-up is shown in Figure 2. The main components were the cover plate, the front plate, the back plate and the supporting frame.



Figure 2 – Rigid test wall alone (left) and installed in the flume (right)

Two configurations of the cover plate were tested one after the other: a flat cover plate and a cover plate with corrugations accurately mimicking the MarkIII membrane corrugations at scale 1:6 with the large corrugations set vertically (see Figure 3). This choice was motivated by the fact that most of the deformed membrane corrugations observed on board ships in the lower part of the tanks, were on the longitudinal bulkheads.

Two instrumented rigid test blocks were embedded into the test wall.

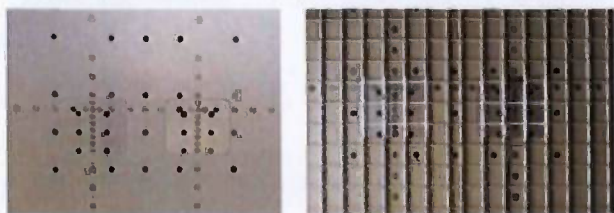


Figure 3 – Flat cover plate (left) and corrugated cover plate (right) with the two test blocks

Pressure transducers with a sensitive membrane of 1.2 mm diameter were installed on the wall as shown in Figure 3 along two vertical lines and a horizontal line. The pressure transducers are described by Bogaert and Kaminski (2010). Locations of the sensors on the vertical line, with

respect to the corrugations within each rigid block are shown in Figure 7 (right).

Each rigid block was mounted on a 6-component load cell.

A special *corrugation sensor* was designed by MARIN in order to measure the net vertical force on a horizontal corrugation segment in between two vertical corrugations (see Figure 4) at the top of the right test block.



Figure 4 – Corrugation sensor alone (left) and as installed on the right rigid block (right)

The data acquisition was sampling at 50 kHz.

Five high speed cameras synchronized with the data acquisition system completed the measurement system. Figure 2 (right) shows the shelters mounted on both sides of the flume near the wall in order to protect both the lighting system and the cameras from the splashes. The shelters assured also a white background for the video recording.

All breaking waves presented in this paper were generated by a focusing technique without any bathymetry (see Kimmoun *et al.*, 2010 and Bogaert, Brosset, Léonard, Kaminski, 2010). Wave packets were generated by the paddle in order to meet at a theoretical *focal point*. The main parameter enabling to adjust the shape of the wave just before the impact was the location of the focal point with regards to the wall. Whatever the type of wave generated, the targeted location for the impact is the horizontal line of pressure transducers at the top of the test blocks (see Figure 3).

IMPACT TYPES

First test campaign performed within SlosheL project at the turn of 2007, was dedicated to *NO96 full scale tests*. Four categories of wave impacts were identified depending on the advancement of the breaking process when hitting the wall (Brosset *et al.*, 2009).

The *SlosheL large scale tests* allowed to reproduce these types of impacts and to get high quality videos of them. Figure 5 shows successive stages of each impact type.

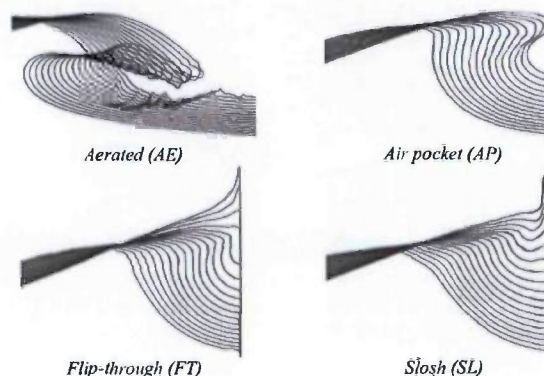


Figure 5 - Four impact types

The free water surface is represented at different times with a constant time step of 5 ms. The shape of the free surface was contoured from the video recordings of the large scale tests with the flat cover plate.

In a flume tank, the generation of these different impact types depends on the position of the focal point with respect to the wall. The waves breaking before hitting the wall (focal point located ahead of the wall) create a lot of bubbles before the impact. This kind of impact is called *aerated impact* (AE). Whatever the adjustment of the paddle signal, the aerated impacts always lead to moderate impact pressures. Their interest is thus limited from a design point of view and they will rarely be mentioned in this paper.

The *air-pocket impact* (AP), *flip-through impact* (FT) and *slosh impact* (SL) correspond to locations of the focal point moving progressively towards the wall and even beyond the wall for slosh impacts. They are the three most important types of wave impacts, inducing significant pressures on a flat wall.

These three impact types remain the same whatever the configuration of the impacted wall (flat or corrugated) is. Figure 6, 8 and 10 show respectively characteristic examples of AP, FT and SL impacts for both a flat wall and a corrugated wall. Figures 7, 9 and 11 give the respective pressure time traces recorded by the different pressure transducers, vertically aligned on one of the test blocks shown in Figure 3.

Statistically, the air pocket and the slosh impacts are more likely to occur because they correspond to a large range of possible focal point locations. Flip-through impacts correspond to a narrow band just in between these two large ranges for AP and SL impacts. Practically a flip-through impact is always a limit case of either a slosh or an air pocket impact.

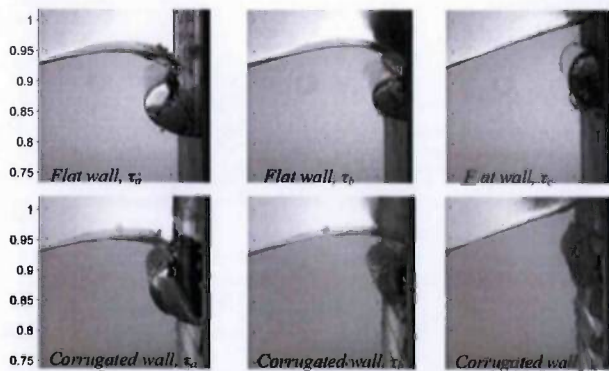


Figure 6 – Air Pocket (AP) impact on flat (top) and corrugated (bottom) walls at three different instants noted τ_a , τ_b , τ_c . Pressure signals given in Figure 7

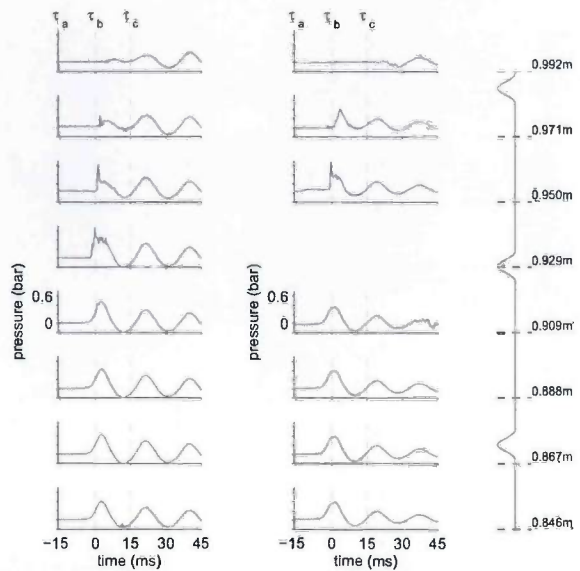


Figure 7 – Pressure profiles for an Air Pocket (AP) impact on flat (left) and corrugated (right) walls. The locations of the pressure sensors are given on the right side. Instants τ_a , τ_b , τ_c refer to the pictures in Figure 6

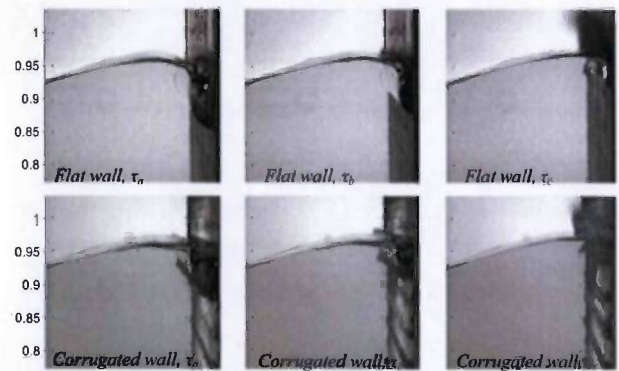


Figure 8 – Flip Through (FT) impact on flat (top) and corrugated (bottom) walls at three different instants noted τ_a , τ_b , τ_c . Pressure signals given in Figure 9.

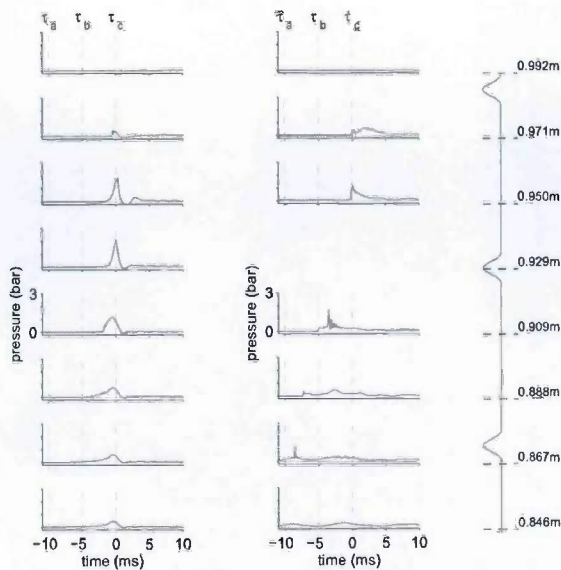


Figure 9 – Pressure profiles for a Flip Through (FT) impact on flat (left) and corrugated (right) walls. Locations of pressure sensors are given on the right side. Instants τ_a , τ_b , τ_c refer to the pictures in Figure 8

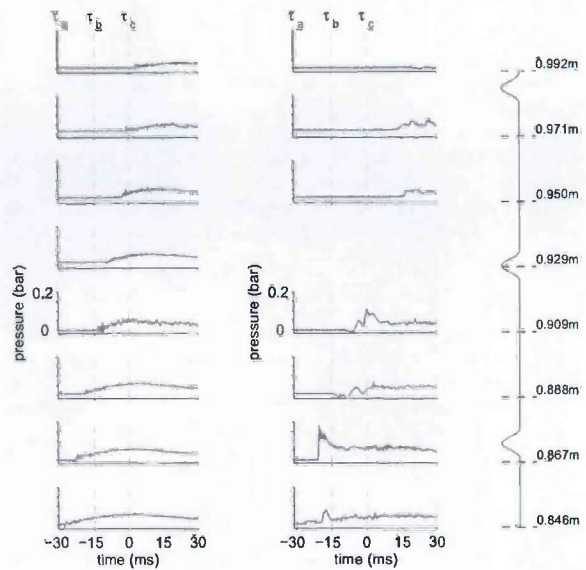


Figure 11 – Pressure profiles for a Slosh (SL) impact on flat (left) and corrugated (right) walls. Locations of pressure sensors are given on the right side. Instants τ_a , τ_b , τ_c refer to the pictures in Figure 10

WAVE – WALL INTERACTIONS

Some general phenomena occur when a travelling wave approaches a wall. These phenomena are the same whatever the configuration of the wall (flat or corrugated) although it is easier to capture them on the videos or the pictures taken with the flat wall.

Run-up process and vertical jet building from the trough

The most general physical phenomenon when a travelling wave is approaching a wall is the run-up process: the wave trough rises progressively along the wall, the free surface remaining perpendicular to the wall. This process enables a transfer of momentum from the horizontal to the vertical direction. It, thus, mitigates the impact. For the slosh waves (see Figure 10 - top), this transfer is complete: all the momentum of the wave is transferred vertically through the run-up process. So, no real impact occurs.

The thickness of the trough is largely reduced when constrained or restricted by the close presence of the wave front. It may become a violent vertical jet fed by the remaining horizontal momentum of the wave front (see Figure 8, top, right). *Restricted troughs* inducing vertical jets occur for impacts very close to flip-through, including small air-pocket impacts or sharp slosh impacts. When a jet is building, there is always a sharp increase of the pressure at its root in the trough area (see Figure 9 - left). For larger air pocket impacts, no vertical jet from the trough is noticed. The trough is not restricted enough and the transfer of momentum happens smoothly. Both the maximum velocity and acceleration of the trough increase in the case of impacts with decreasing sizes of air pockets.

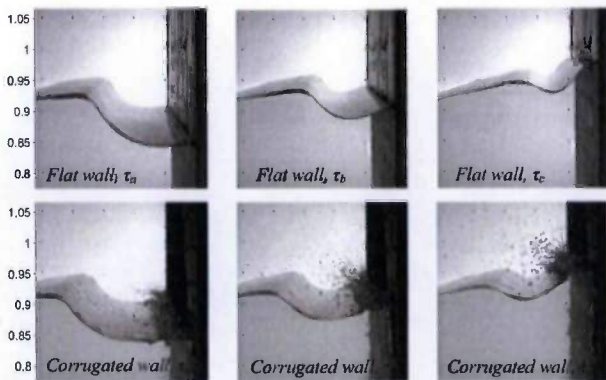


Figure 10 – Slosh (SL) impact on flat (top) and corrugated (bottom) walls at three different instants noted τ_a , τ_b , τ_c . Pressure signals given in Figure 11

Pulsating Air pocket

For AP impacts, an air pocket is entrapped between the trough, the crest and the wall (see Figure 6). The pocket closes when the crest hits the wall. The air pocket is pressed by the wave front, which still keeps some horizontal momentum, and the wave trough running up. The pocket acts like a spring, the stiffness of which is given by the compressibility modulus, compressed by water inertia. The volume of the air pocket oscillates together with the pressure inside. All pressure sensors within the gas pocket give exactly the same pressure signals (see Figure 7 – left – 4 lowest sensors). The pocket main trajectory is driven by the upward general motion starting from the trough run-up.

Crest impact and vertical jets building from the crest

For air pocket impacts, the horizontal momentum cannot be completely transferred to the trough run-up process. A crest is building progressively and hits the wall (see Figure 6 - top). Despite the presence of the gas around the crest that will take a part of the crest momentum when forced to escape, a real impact happens. A sharp peak pressure is observed just in front of the crest that superimposes to the low frequency oscillating pressure from the gas pocket (see Figure 7 left, sensor at 0.950 m). As already noticed during the full scale tests (see Brosset *et al.*, 2009), this sharp peak pressure is much localized. The density of installed pressure sensors is not high enough to guaranty an accurate capture of this peak for each crest impact. After contact a vertical jet is ejected upward (see Figure 6 – top – middle). A vertical jet may also be expelled downward inside the air pocket but was not detected from the videos.

Summary

Depending on the impact type (AP, FT or SL), the wall (flat or corrugated) can potentially be loaded by three different parts of the wave: the trough, the crest and the pocket. Figure 12 summarizes the different possibilities.

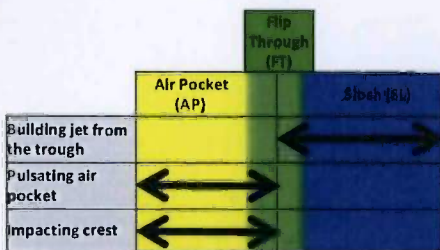


Figure 12 – Different kinds of loads from the wave-wall interaction

WAVE – CORRUGATION LOCAL INTERACTIONS

The different sources of loading due to the wave-wall interaction remain when the wall is corrugated. They load the containment system in between the corrugations. However, each part of the wave (trough, pocket and crest) interacts with the corrugations differently, which may lead to local mitigation or enhancement of the loads in between the corrugations compared to what would be obtained on a flat wall. This wave-corrugation local interaction also leads to specific loading mechanisms of the corrugations. The different types of local interactions are sorted out by the part of the wave which is involved.

The study is focused on horizontal corrugations as the loads obtained on vertical corrugations are of no interest when considering unidirectional waves. In this section, only the phenomena are described.

The results in terms of loads on the corrugations or on the flat areas are shown in the two next sections.

Wave trough - corrugation interaction (I)

During the run-up of the trough along the corrugated wall, the trough hits each horizontal corrugation, separates from the wall and reattaches downstream of the corrugation afterwards, before hitting the next corrugation. When the trough is restricted, a jet may surge and hit the corrugation above.

A trough located in cell n between corrugation n and corrugation $n+1$ loads: (1) corrugation n , (2) cell n and/or (3) cell $n+1$. When a cell is loaded, the polyurethane foam below the membrane would be loaded in the reality. Corrugation and cell loadings are respectively referred to as *CRG* and *CCS* loadings.

While entering into the liquid during the trough run-up, the lower side of the horizontal corrugation n is loaded (I-1_CRG). The cell n underneath the loaded corrugation n is loaded locally at the same time (I-1_CCS), especially in the case of a restricted trough. This leads to an enhancement of the pressure upstream of the corrugation. When reattaching to the wall, the flow loads cell $n+1$ (I-2_CCS).

Figure 13 shows this process (I-1, I-2) for both an unrestricted trough (top) and a restricted trough (bottom).

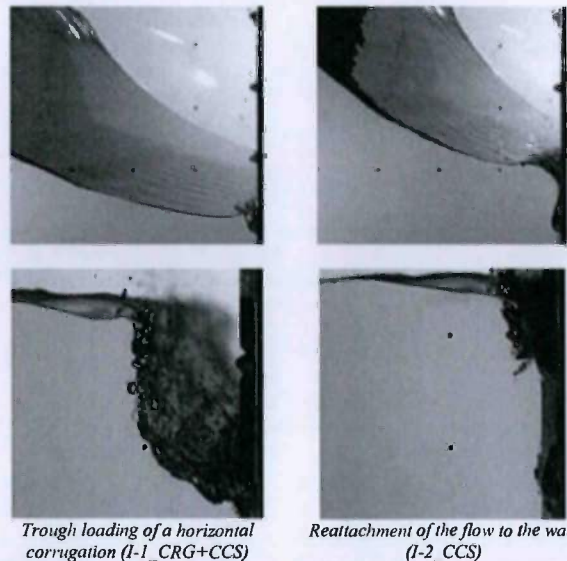


Figure 13 – Wave trough – corrugation interactions, Loading mechanisms I-1 (left) and I-2 (right) (see Table 1) - Unrestricted (top) and restricted (bottom) troughs

It is apparent in Figure 13 that the trough remains horizontal in the area close to the wall.

The velocity and the acceleration of the trough are much higher for the impact conditions corresponding to a restricted trough. Therefore the trough loading on horizontal corrugations is expected to be much higher for a restricted trough obtained for focal point locations close to the flip-trough conditions than for an unrestricted trough obtained with large air-pocket impacts.

Furthermore, when the trough is restricted, the run-up along cell n may feed a thin vertical jet with high vertical velocity. This jet hits the lower side of the above horizontal corrugation n as shown in Figure 14. This corrugation loading mechanism (I-3_CRG) is linked to an enhancement of the pressure upstream of the corrugation (I-3_CCS). Figure 11 shows

such an enhancement of the pressure, measured upstream of a horizontal corrugation by the sensor located at 0.867 m, for a jet induced by a slosh impact.

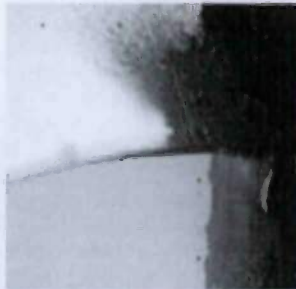


Figure 14 – Jet loading (I-3) of a horizontal corrugation induced by a restricted trough

Air-pocket - corrugation interaction (II)

There is no special phenomenon induced by the presence of a corrugation when located inside an air pocket of an AP impact (Figure 6 – bottom – middle). The pressure inside the air pocket can be considered as uniform. Any part of a corrugation inside the air pocket is loaded with that pressure. Most of the time, both sides of the corrugation inside an air pocket are loaded in the same way, symmetrically (II-1_CRG). The net vertical force on a horizontal corrugation is therefore negligible. The corrugation may be crushed but not bent.

A corrugation at the boundary of an air pocket is loaded non-symmetrically (II-2_CRG). This kind of loading tends to bend the corrugation.

In both cases, the cell inside the gas pocket is loaded approximately by the same pressure with or without corrugated membrane on the wall for the same steering signal of the paddle, as illustrated by Figure 7 for the four lowest pressure transducers located inside the air-pocket.

Wave crest - corrugation interaction (III)

The wave crest may hit directly a corrugation as shown in Figure 15 (left) and load more or less equally both sides (III-1_CRG). This depends on the relative position between the crest and the corrugations.

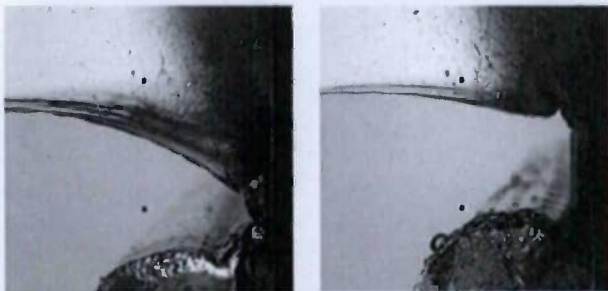


Figure 15 – Crest loading of a horizontal corrugation (III-1) and resulting jet loading of the next upper horizontal corrugation (III-2)

After that, the crest reaches both cells around the corrugation. The cell is loaded at the shoulders of the corrugation (III-1_CCS).

Whatever the location of the crest in the cell n (including corrugation $n-1$) when hitting the corrugated wall, a violent vertical jet starts upward from the contact point and hits, thus loads (III-2_CRG), the next horizontal corrugation above n as shown in Figure 15 (right). The

pressure upstream of the corrugation may be magnified at the same time (III-2_CCS). Figure 7 shows such an enhancement measured upstream of a horizontal corrugation by the pressure sensor located at 0.971 m for an AP impact.

Summary

For a given impact type, the different parts of the wave interact with the horizontal corrugations. Table 1 summarizes the different loading types on corrugations (referred to as CRG) and on the flat membrane (referred to as CCS for containment system) which were identified in this section.

Table 1. – Wave – horizontal corrugation local interaction. CRG=corrugation loading – CCS=Flat membrane loading change

Wave part	Loading description	Code	CRG	CCS
Trough	Run-up (water entry)	I-1	CRG	CCS
	Flow Reattachment	I-2		CCS
	Jet from restricted trough	I-3	CRG	CCS
Pocket	Pocket not limited by a CRG	II-1	CRG	
	Pocket limited by a CRG	II-2	CRG	
Crest	Crest impact	III-1	CRG	CCS
	Jet from crest	III-2	CRG	CCS

The main types of corrugation loading are the wave trough loading, the crest loading and the jet loading. The jets are induced either from a restricted trough or a crest impact.

CORRUGATION LOADING

Figure 16 shows the maximum vertical forces measured by the corrugation sensor shown in Figure 4, for all Sloshe tests at scale 1:6. The result of each test is classified according to the impact type (AE, AP, FT, SL) and the local type of corrugation loading (trough, crest or jet).

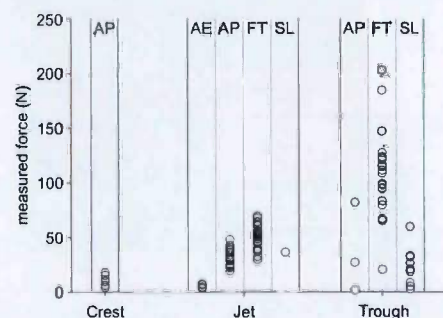


Figure 16 - Measured force on horizontal corrugation. Subdivision made per aerated (AE), air pocket (AP), flip-through (FT) and slosh (SL) impact.

As already mentioned, the corrugation sensor is only able to measure a net vertical force. So a pressure equal on both faces of the corrugation leads to no force measured. As the crest loading type (III-1) of the corrugations potentially loads both sides of the corrugations, the corrugation sensor is not relevant for measuring it. On the contrary, as jets (I-3 & III-2) or wave trough (I-1) load only the lower side of the corrugations, the corrugation sensor is very relevant for capturing them.

The highest vertical force on the horizontal corrugation was obtained for trough loading (I-1). Actually only troughs restricted by a close wave front lead to significant vertical forces on the corrugation. This

happens for impact types that are very close to flip-through although impacts some of them can still be labelled as slosh impacts or small air pocket impacts.

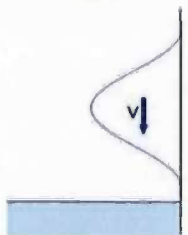


Fig. 17 – Water entry problem

The impact corresponding to the maximum force of 203 N (scale 1:6) is a flip-through shown in Figure 13 (bottom). It is tempting to consider this kind of trough loading as a water entry problem governed by the vertical trough velocity (see Figure 17). The maximum trough velocity in this case was evaluated from the high speed video as 15 m/s. A generalized Wagner theory as proposed by Zhao and Faltinsen (1996) and implemented by Scolan (Scolan, 2008) leads to an evaluation of the maximum force around 20 N.

Such a simplified vision of the wave trough loading by a water entry problem of the corrugation into a flat free surface seems to be inadequate, at least for a wave trough loading. Further investigations are to be made for unrestricted trough loading.

Jets induced either by the wave crest (III-2) for AP impacts or by the wave trough (I-3) for FT or SL impacts may also lead to high vertical forces though smaller than for wave trough loading. The maximum recorded force from a jet is 64 N (scale 1:6) obtained for FT impact. Figure 18 shows this FT impact and the jet induced by the restricted wave trough hitting the corrugation.

Actually, the test matrix was built so as to measure the maximum force or pressure. It means that the parameters, including the relative location of the point of impact versus the corrugation sensor, were adjusted more carefully for restricted trough loading than for jet loading. Consequently higher forces on the corrugation could have been obtained for jet loading (either I-3 or III-2) with the same waves by adjusting the impact location with respect to the horizontal corrugations.

It can be noted that the only forces measured by the corrugation sensor for AE impacts were jet impacts with low forces. This confirms that AE impacts can be disregarded when corrugation loading is considered.

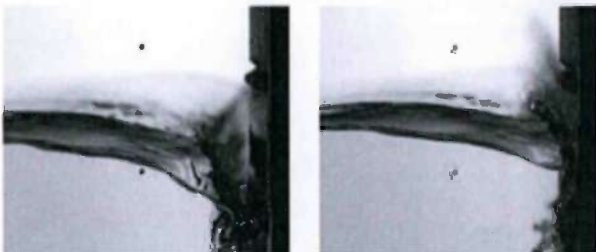


Figure 18 – Flip-through impact inducing the maximum jet loading (64 N) on the corrugation sensor, 5 ms between the two pictures.

From the force measured by the corrugation sensor one can define a mean pressure on the largest section of the corrugation. As the cylindrical part of the horizontal corrugation has a width of $(340-70)/6 = 45$ mm and a height of 7 mm (for technical reasons a little higher than the actual scaled height $37.2/6 = 6.2$ mm), the largest section considered is 315 mm^2 . It is interesting to compare this mean pressure to the pressure measured by the transducer upstream of the corrugation sensor. The projected distance between the pressure transducer and the corrugation apex is 15.4 mm. The apex is located at a height of 986.4 mm.

Figure 19 presents the results with the same classification of corrugation loadings and subdivisions of impact types as in Figure 17.

Pressures are given at model scale and at full scale considering a Froude-scaling with LNG (430 kg/m^3) instead of water (1000 kg/m^3). Froude-scaling is proposed here because often used and no better suggestion is ready.

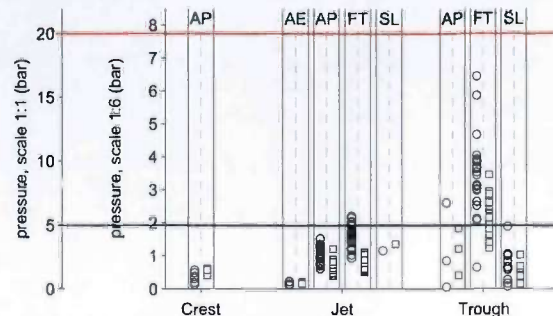


Figure 19 – Maximum mean pressure from the corrugation sensor (○) and maximum pressure upstream of the corrugation (◻). Subdivision made per aerated (AE), air pocket (AP), flip-through (FT) and slosh (SL) impact. Scale 1:1 pressures are Froude scaled with LNG instead of water.

It is clear that the pressures measured upstream of the corrugation are lower than the mean pressures on the corrugation for the most significant impacts. The maximum pressure at the basis of the corrugation is probably not captured by the closest lower sensor due to its being too far from the corrugation. This result is further developed in the next section concerning the containment system loading.

After the incidents with the MarkIII membrane in LNG carriers in 2008, GTT carried out investigations which concluded that up to a static pressure of 20 bar, both the corrugations and the insulation below remain sound even though the corrugations may be significantly deformed. For a first visible deformation of the small corrugation, a static pressure of 5 bar is required.

These two pressure thresholds are represented on Figure 19 by a black (5 bar) and a red (20 bar) lines. It is to be noticed that no impact was generated, despite our good will, leading to a corrugation loading above the damaging limit established by GTT. On the contrary many would have led to a permanent visible deflection of the horizontal corrugations. It is unfortunately not possible to determine what the probability of occurrence of such impacts is from the data base. The large number of high pressure impacts obtained only reflects the will of the Slossel partners to focus on these kinds of impacts. Nevertheless most of these high pressure impacts were obtained for flip through impacts which can be considered as a condition being difficult to adjust in a lab and unlikely to happen with 3D real excitations.

These high loads of the horizontal corrugation are obtained by trough or jet loadings of the lower side of the corrugation. They would lead to asymmetric deflection (local or global bending) of the corrugation.

Crest and air-pocket loadings are the only kinds that could explain pinching deflection of the horizontal corrugations that were observed on board MarkIII ships. The highest pressure measured upstream of the horizontal corrugation sensor for crest loading is much lower than the threshold for a visible permanent deflection. This may only be due to the fact that the sensor was too far from the corrugation to capture the maximum pressure. An improved corrugation sensor was developed for the Slossel full scale tests with the MarkIII membrane. These tests have already been performed in April 2010. The new sensor is able to measure both the upward and the downward vertical forces on the horizontal corrugation.

The results of these full scale tests should answer the question whether crest impacts are able to pinch permanently a horizontal corrugation.

The maximum pressure measured inside a gas pocket is 1.3 bar, which is much below the threshold inducing a first visible deformation.

Studying unidirectional waves does not allow capturing high asymmetric loads on the vertical corrugations. Nevertheless crest and air-pocket loadings are potentially able to pinch as well a vertical corrugation as a horizontal one. So, conclusions remain the same on the vertical corrugations for this kind of symmetrical loadings.

CONTAINMENT SYSTEM LOADING

In the previous section the focus was on the loads on the corrugations of the MarkIII membrane. Considering the excellent fatigue behaviour of the membrane, even after strong deflections of the corrugations, this part is not the most essential for the safety of the ship. The focus is now on the loads on the flat areas of the membrane in between the corrugations that would load directly the polyurethane foam of the MarkIII containment system on board LNG carriers.

The analysis of the containment system loading is difficult for several reasons:

- The density of sensors on the test blocks was too low to capture adequately the highest sharp peaks (Kimmoun *et al.*, 2010). In particular, as seen in the previous section (Figure 19), the measured pressures just upstream of the corrugations in the impact areas are likely to be underestimated.
- The impact types inducing the highest local pressures (Figure 19) are the flip-through impacts. These impacts are limit cases of air-pocket impacts, for which the pocket volume tends towards zero. They are very sensitive to the initial conditions. Consequently, even when repeating carefully the same paddle steering signal adjusted for the flip-through conditions, even if the wave had been especially studied in order to give the best repeatable results, the results in terms of measured pressures were largely spread (see Kimmoun *et al.*, 2010 and Bogaert, Brosset, Léonard, Kaminski, 2010).
- The flip-through impacts are conditions helping to understand the physics of wave impacts, but considered as unlikely to occur in real situation with 3D ship motions.
- The large scale tests were done at scale 1:6 and scaling of the corrugations influence is not mastered.

Nevertheless, after all these reminders, some interesting trends can be derived from the large scale data base.

Four air-pocket, seven flip-through and four slosh impact conditions were repeated with the same paddle steering signals for both the flat and the corrugated walls. The results presented in this section compare directly the couples (flat/corrugated) of maximum loads, namely local pressures or mean force on the two test blocks (see Figure 3), for these conditions in order to show the influence of the corrugations on the CCS loading.

Figure 20 shows scatter plots of the maximum measured forces, perpendicular to the wall, on the test blocks. The abscissa and ordinate are respectively the values obtained on the flat wall (FW) and on the corrugated wall (CW). The shapes and colours of the dots indicate the kinds of wave impacts (AE, AP, FT, SL).

The results for flip-through impacts are significantly spread and do not show a general trend. Indeed their high variability to the initial conditions masks the phenomenon that one tries to analyse, even for global force measurements supposed to be more stable than local pressures. For slosh and air-pocket impacts, slightly higher loads can be observed on the corrugated wall than on the flat wall. A closer look to the local loads for these two impact types is necessary.

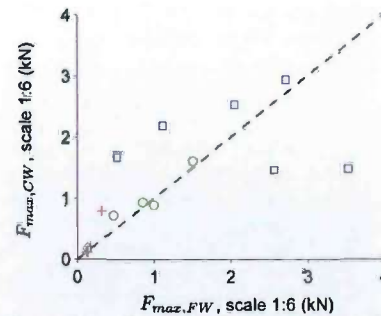


Figure 20 – Comparison of the max. forces on the test blocks, recorded on the flat (F_{FW}) and the corrugated (F_{CW}) walls for the same wave paddle signal. Aerated (\diamond), air pocket (\circ), flip-through (\square) and slosh ($+$)

Figure 21 shows for SL and AP impacts, the ratio P_{CW}/P_{FW} of the maximum pressure obtained on the corrugated wall (P_{CW}) to the maximum pressure obtained on the flat wall (P_{FW}) for the same location along the middle vertical of the test blocks and the same paddle excitation. Locations of the corrugations are represented with red lines.

These plots are to be analysed carefully: a high ratio P_{CW}/P_{FW} may correspond to a small reference value. So, the maximum value of P_{CW} and P_{FW} are displayed on each sub-figure.

A general trend of higher local pressures is clearly observed for the corrugated wall. Also, the details considering the part of the wave involved and the location of each sensor with regards to the next downstream corrugation, thus the kind of wave-corrugation local interaction (see Table 1), make sense.

For the slosh type of impacts (Figure 21 – left) the lowest corrugation within the test block interacts with the trough when it runs-up and the jet is building up (instant τ_a in Figure 10 - bottom). The overpressures observed on Figure 21 are thus of the same kind as those described on Figure 11 for the sensor at 0.867 m from the bottom (I-1 or/and I-3 in Table 1). The sensor upstream of the top corrugation captures also significantly larger pressures due to the jet hitting this corrugation (I-3).

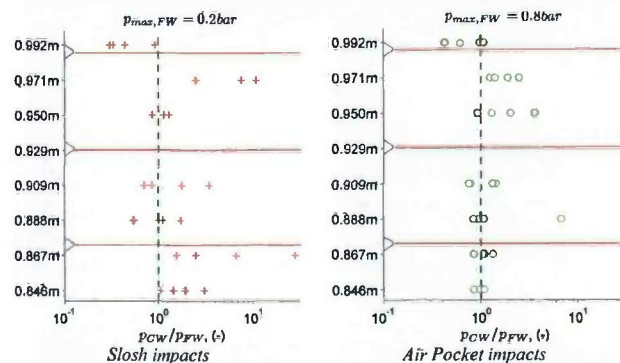


Figure 21 – Comparison of the max. pressure on corrugated and flat walls at the same location for the same wave paddle signal

For the air-pocket type of impacts (Figure 21 – right), the crest is most of the time hitting the wall between the corrugations at respectively 0.929 m and 0.992 m above the bottom. The increase of pressure for the corrugated wall at sensors at 0.950 m and 0.971 m above the bottom are related to the jet-from-the-crest hitting the top corrugation (III-1) as observed in detail for a particular air-pocket impact in Figure 7.

For both the slosh and the air-pocket impacts, a reduction of the pressures is observed just above the top corrugation when using the corrugated wall. This effect must be much localized, because the sensors respectively at 0.950 m and 0.888 m just above other corrugations but a little further do not show this effect.

The overpressures observed must be also much localized at a given moment since the force magnification observed in Figure 20 remains small.

DOES IT MAKE SENSE TO PERFORM MODEL TESTS WITH CORRUGATIONS?

The two previous sections have shown that the wave – corrugation local interactions have a significant influence on both the corrugation loads and the containment system loads. How can this influence be taken into account within a sloshing assessment based on model tests? Would it be an improvement, though technically challenging, to perform small scale tests with scaled corrugated walls in the areas of impacts?

Sloshing model tests as performed in GTT are based on the use of model tanks at scale 1:40. Let us imagine a scale 1:34 in order the distance between two consecutive parallel corrugations (large or small) is 1 cm. Heights of large and small corrugations would thus become respectively 1.6 mm and 1.1 mm at small scale. Assuming the fabrication of the corrugations at scale technically possible, it may be feasible after changing the sensor housings, to set-up four SlosheI pressure sensors (these sensors have a particularly small sensitive membrane area (1.3 mm diameter)) within one cell.

In order to derive reliable full scale loads at least on the containment system two requirements are necessary to be fulfilled:

- the wave – corrugation local interaction must be *similar* at both scales
- the measured pressures are representative of the maximum loads

The first condition is unlikely to be fulfilled because with such a small size of the corrugations at small scale, viscous effects governed by Reynolds number or tension surface effects governed by Weber number are expected to have a strong influence.

Furthermore, according to SlosheI large scale tests, the second requirement is not fulfilled. Indeed, the measured pressures depend highly on the distance between the sensor upstream of the corrugation and the corrugation itself. For example, the closest lower sensor to the top corrugation within the test block was not able to capture the maximum pressure at the root of the corrugation, which should be larger than the mean pressure on the corrugation largest section, derived from the force measurement on the corrugation (see Figure 19). The projected distance between this sensor and the corresponding corrugation was 21 mm at scale 1:6. Geometrically scaled at scale 1:34, it would become 3.7 mm. So, the results of the model tests would highly depend on the minimum distance the sensor could be positioned with regards to the adjacent corrugation.

Figure 22 illustrates this influence of the distance between a sensor upstream of an adjacent corrugation and the corrugation itself. The maximum pressure measured upstream the corrugation ($p_{max,UC}$) is compared to the average pressure derived from the force measured by the corrugation sensor (p_{AVG}). The two most significant types of corrugation loadings (trough run-up loading (I-1) and jet loading (I-3 and III-3)) are displayed separately. Different impact types are distinguished by using different colours and symbol shapes.

For a given distance (here 15.4 mm) between the sensor and the corrugation, the underestimation of the maximum pressure at the root of a corrugation is significant and depends on the impact type and the wave-corrugation local interaction type.

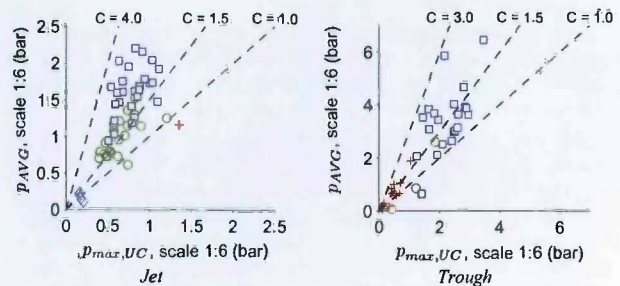


Figure 22 – Average pressure on corrugation (p_{AVG}) and maximum pressure upstream of corrugation ($p_{max,UC}$). Aerated (\diamond), air pocket (\circ), flip-through (\square) and slosh (+) impacts

CONCLUSIONS

After the NO96 full scale wave impact tests carried out at the turn of 2007, the SlosheI consortium performed large scale wave impact tests in April 2009 at scale 1:6 in a smaller facility. The objectives of the new tests were multiple:

- Study the scaling effects by mimicking at large scale the waves generated first at full scale, when impacting a flat rigid wall. Bogaert, Brosset, Léonard, Kaminski, (2010) present the findings.
- Prepare MarkIII full scale wave impact tests by tests on both a flat and a corrugated wall in order to:
 - ✓ improve the quality of the waves for better mastering the repeatability of the waves developments and of the pressure measurements (Kimmoun *et al.*, 2010 and Bogaert, Brosset, Léonard, Kaminski, 2010).
 - ✓ obtain design loads for the MarkIII full scale set-up.
 - ✓ obtain a data base with the corrugated wall and conditions to be repeated at full scale during the Mark III tests in order to study the scaling effects on the corrugated wall.

MarkIII full scale tests were performed in April 2010 but have not been analysed yet. The present paper is limited to the findings from the large scale tests and the comparison of results obtained with the corrugated wall and with the flat wall. The three main categories of impacting waves (air-pocket, flip-through and slosh impacts) already studied in NO96 full scale tests were studied again.

High speed video recordings synchronized with the pressure acquisition enabled an analysis of the phenomena when a wave interacts with a flat wall. The wall is loaded by the impacting crest, the compressed air pocket and the root of the jets building up either from the trough during the run-up process or from the crest after its impact. The loading of the jet is due to the local change of direction of the liquid momentum.

These general wave-wall interaction phenomena remain when the wall is corrugated, but in addition, they interact with the corrugations generating specific loadings of the corrugations and modifying locally the loading in between the corrugations. Six different loading mechanisms were observed involving either the corrugations or the cells, thus the polyurethane foam in the reality on board ships.

The maximum loads were obtained with flip-through impacts, difficult to adjust in laboratory and therefore not considered as likely with real 3D ship motions. However, maximum force recorded on a horizontal corrugation during the whole test campaign would not have damaged the corrugation nor the foam below at full scale, according to Froude scaling.

Nevertheless, several air-pocket and slosh impacts, considered as more likely to occur in the reality, induced a mean pressure which could have

led to permanent visible deformations at full scale.

Several mechanisms were observed inducing an enhancement of the pressures locally just underneath the horizontal corrugations in the impact areas. A too low density of pressure transducers in the impact area was used to capture the highest pressure peaks.

In addition to the scaling difficulties, this high density of sensors required in between two corrugations is the reason why the authors do not recommend to model the corrugations during sloshing model tests.

All results obtained from the large scale tests, thus at scale 1:6, have to be confirmed from the MarkIII full scale tests, whereby not only the scale was changed, but the test conditions were improved. In particular, a higher density of pressure sensors covered the two test blocks.

ACKNOWLEDGEMENTS

The views expressed in the paper are those of the authors and do not necessarily represent the unanimous views of all the consortium members.

The authors would like to acknowledge the support provided by the Sloshel consortium members that have made the Sloshel project possible: American Bureau of Shipping, Bureau Veritas, Ecole Centrale Marseille, Chevron, ClassNK, GTT (Gaztransport & Technigaz), Lloyd's Register, MARIN and Shell.

The support provided by the subcontractor Deltares is appreciated.

REFERENCES

Bogaert, H., Brosset, L., Léonard, S., Kaminski, M.L., (2010), "Sloshing and scaling: results from Sloshel project", 20th (2010) Int. Offshore and Polar Eng. Conf., Beijing, China, ISOPE, Vol 3.

Bogaert, H., Léonard, S., Marhem, M., Leclère, G., Kaminski, M.L., (2010). "Hydro-structural behavior of LNG membrane containment systems under breaking wave impacts: findings from the Sloshel project", 20th (2010) Int. Offshore and Polar Eng. Conf., Beijing, China, ISOPE, Vol 3, www.isopec.org.

Bogaert, H., Kaminski, M.L., (2010) "Advances in sloshing assessment from the Sloshel project", 20th (2010) Int. Offshore and Polar Eng. Conf., Beijing, China, ISOPE, Vol 3, www.isopec.org.

Brosset, L., Mravak, Z., Kaminski, M.L., Collins, S., Finnigan, T., (2009) "Overview of Sloshel project", 19th (2009) Int. Offshore and Polar Eng. Conf., Osaka, Japan, ISOPE, Vol 3, www.isopec.org.

Gervaise, E., de Sèze, P.E., Maillard, S., (2009) "Reliability-based methodology for sloshing assessment of membrane LNG vessels", 19th (2009) Int. Offshore and Polar Eng. Conf., Osaka, Japan, ISOPE, Vol 3.

Kaminski, M.L. and Bogaert, H. (2010). "Full Scale Sloshing Impact Tests -Part 1," Int J Offshore and Polar Eng, ISOPE, Vol 10, No 1.

Kimmoun, O., Ratouis, A., Brosset, L., (2010) "Sloshing and scaling: experimental study in a wave canal at two different scales", 20th (2010) Int. Offshore and Polar Eng. Conf., Beijing, China, ISOPE, Vol 3.

Scolan, Y.-M., (2008) "Rapport d'étude sur l'écoulement autour de corrugation de type MarkIII", Rapport Gaztransport & Technigaz, October, 2008.

Zhao, R., Faltinsen, O., Aarsnes, J., (1996) "Water entry of arbitrary two-dimensional sections with and without flow separation", 21th Symp on Naval Hydrodyn.

Copyright ©2010 The International Society of Offshore and Polar Engineers (ISOPE). All rights reserved.